Congshan Li, Pu Zhong, Ping He*, Guixian Yang, Yuqi Ji

J. Electrical Systems 17-3 (2021): 298-309

Regular paper

Fast identification of internal and external faults of HVDC transmission line based on frequency spectrum correlation

This paper presents a new method for rapid detection of internal and external faults on HVDC transmission line based on frequency spectrum (FS) correlation. Due to different physical boundaries consisted of DC filters, smoothing reactors and DC line distributed capacitance, the transient DC current signals of internal and external faults have different amplitude frequency characteristics, which constitute the intrinsic feature of its inherent. The FS characteristics of the DC current signals can be obtained via discrete Fourier analysis method. First, a set of eigenvector defined as eigen frequency spectrum eigenvector (EFSE) is formed including four types of intrinsic FS scenarios which are: normal operation, internal fault, external fault local side (EFLS) and external fault opposite side (EFOS). Second, the same method is utilized to obtain the FS of DC current of any fault, and the similarity coefficients between the FS and eigen frequency spectrum (EFS) are calculated. Thus, the fault type can be identified by comparing the magnitude of similarity coefficients of the FS and EFS. The fault type corresponding to the maximum similarity coefficient is the product of the judgment. Finally, a large number of fault simulations are performed on the PSCAD simulation platform and the effectiveness and robustness of the proposed method are verified.

Keywords: HVDC, internal and external faults, eigen frequency spectrum, similarity coefficient, dynamic permutation entropy, Fourier analysis.

1. Introduction

Fast and accurate fault identification is the inevitable requirement of smart grid [1]. As a long-distance transmission system, HVDC often needs to cross rough terrains such as snow-capped mountains, rivers, etc. Therefore, the fault probability of DC transmission line is generally higher [2,3]. Fast identification of internal and external faults of HVDC transmission line is a precondition for system protection and operation. The traveling wave protection of DC transmission line based on the voltage change rate of *du/dt* is affected by transition resistance. Therefore, when the system has high resistance grounding fault, it often cannot effectively distinguish internal faults and external faults [4-8]. The discriminative characteristic in the backward traveling wave between the internal and external faults is studied in [9], thus, the fault can be identified. By calculating the correlation coefficients of voltage theoretical value and measured value, a method to distinguish internal from external faults is studied in [10]. It can realize the internal and external faults diagnosis. However, the voltage theoretical value requires the parameter data of the transmission line. As a result, this method is affected by parameter uncertainties. Both sides of the physical boundary of HVDC systems consist of different DC filter, smoothing reactor. Consequently the frequency distribution characteristics of the DC current signal are obviously different between normal operation and various fault conditions. The transient characteristics of the DC current are studied in [11], and a multi-fractal spectrum method is suggested to distinguish the internal and external faults. Nevertheless, this method can't distinguish the EFLS and EFOS. Ref. [12] uses multi resolution singular spectrum entropy and support vector machine to distinguish the internal

* Corresponding author: Congshan Li, Pu zhong, Ping He, School of Electrical and Information Engineering, Zhengzhou University of Light Industry, Dongfeng Road No.5, Zhengzhou, 450002, China, E-mail: 2015018@zzuli.edu.cn, 807393978@qq.com, 9036943@qq.com, 410778909@qq.com, 764468719@qq.com.

from external faults. As the support vector machine is an intelligent classification method, it requires large number of data samples which may not be feasible. Ref. [13] proposes a hybrid traveling wave distance and boundary protection method, in which the wavelet transform is used to deal with the distortion of the boundary. The difference of the transient voltage wavelet energy and the difference of high frequency transient voltage of internal and external faults are used to construct the fault criterion [14,15], obviously, both methods are also affected by the transition resistance. Besides, harmonic current protection is proposed based on boundary characteristics in [16,17].

Based on the above researches, a novel fast identification method of internal and external faults on HVDC transmission line by FS correlation is proposed in this paper. First, the FS characteristics of the DC current signal is obtained by using discrete Fourier analysis method by decomposing the signal and removing the DC component of the signal. Then, a set of eigenvector defined as eigen frequency spectrum (EFS) is formed which includes four kinds of intrinsic FS: normal operation, internal fault, EFLS and EFOS. Second, the same method is utilized to obtain the FS of DC current of any fault, and the similarity coefficients between the FS and EFS are calculated. Finally, the fault can be identified by comparing the similarity coefficients of the FS and EFS. The fault corresponding to the maximum similarity coefficient is the product of the judgment.

In this paper, permutation entropy algorithm is used as the starting condition of the discriminant program, which can avoid the protection from maloperation. The internal and external faults identification of HVDC transmission line based on frequency spectrum (FS) correlation is not affected by the fault transition resistance. Compared with the existing methods, this method not only requires little electrical quantity information, but also can meet the rapidity and selectivity requirements. A large number of HVDC faults are simulated on the PSCAD simulation platform to verify the feasibility and robustness of the proposed method.

2. Internal and external physical boundary and amplitude frequency characteristics

When internal and external faults occur in a DC transmission line, the frequency components of the DC current vary greatly [13]. A physical boundary consists of the smoothing reactor and the DC filter [18]. An unipolar DC transmission system shown as an example in Fig.1.

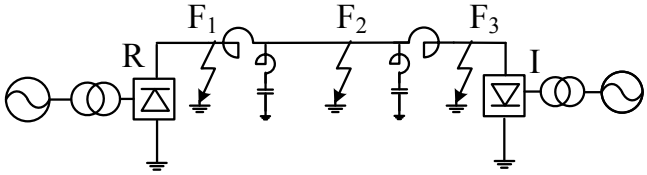

Fig.1. Unipolar HVDC system

The DC current signal measured by the protection device at the inverter side is chosen as the analytical subject. Suppose an external fault occurs at the rectifier side (i.e. opposite side) located at F_1 in Fig.1. The physical boundary of the transient current passed through to the protection location is illustrated in Fig.2 (a).

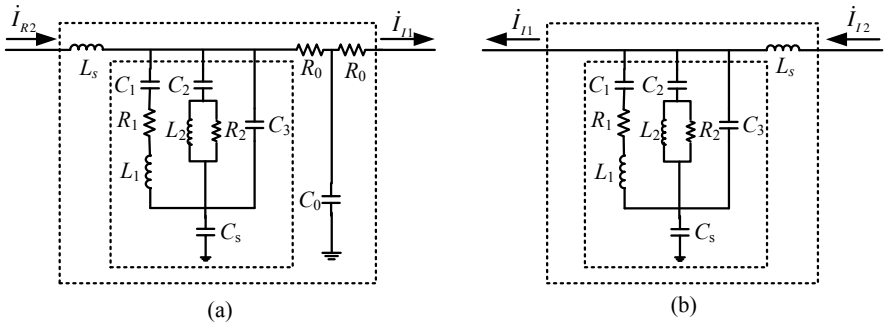

Fig.2. Physical boundary
(a)Opposite side; (b) Local side

In Fig.2 (a), L_s is smoothing reactor on the rectifier side; R_0, C_0 are the resistance and the ground capacitance of DC transmission line; the inner dashed box is the filter bank of the rectifier side. Thus, the physical boundary consists of DC smoothing reactor, DC filter and an entire DC transmission line. Suppose an external fault occurs at the inverter side (i.e. local side) located at F_3 in Fig.1, the physical boundary of the transient current passed through to the protection location is shown in Fig.2 (b).

In Fig.2 (b), Ls is a smoothing reactor on the inverter side. The inner dashed box is the filter bank on the inverter side.

Through the above analysis, it can be observed that the main difference of the physical boundary between the external rectifier side and the external inverter side is the DC line parameters. Due to the existence of distributed capacitance and inductance of the DC transmission line, the DC current signal is filtered to a certain extent. Thus, it leads to differences in terms of the frequency components contained in the DC current signal measured at the protection devices.

In order to compare the frequency characteristics caused by the difference physical boundary, this paper makes use of the measurement data and the total least squares-estimation of signal parameters via rotational invariance technique (TLS-ESPRIT) identification method [19]. Disconnect the power supply on both sides and apply the excitation power supply at one end of the component in Fig.2, and the other end is grounded. The input voltage and output voltage signals are measured, and the transfer functions of the side and the opposite side are obtained as follows:

$$G_1(s) = -7.3\times10^5 \times \frac{1+0.007\cdot s}{s\cdot(1+12.08\cdot s)(1+0.048\cdot s)} \tag{1}$$

$$G_2(s) = -12.62\times \frac{1+0.71\cdot s}{s\cdot(1+0.022\cdot s)(1+0.012\cdot s)} \tag{2}$$

$$G_3(s) = 3.2\times10^{-6} \times \frac{1+8\times10^5\cdot s}{s\cdot(1+0.001\cdot s)(1+0.001\cdot s)} \tag{3}$$

where $G_1(s)$, $G_2(s)$ and $G_3(s)$ respectively denote the transfer functions of internal, external rectifier side and external inverter side. The amplitude frequency characteristics curves are obtained according to these transfer functions.

From Fig.3 (a) and Fig.3 (b), it can be found that, regardless of the fault location (on the local side or on the opposite side), the smoothing reactor and DC filter have a significant

effect on the attenuation of high frequency signals. Comparing Fig.3 (a) and Fig.3 (b), it can be seen that the attenuation of the high frequency signals of DC current of the EFOS is obviously higher than the EFLS. This is due to the existence of DC line capacitance. This difference is caused by the characteristics of the line itself and is not affected by other unknown interference factors. Therefore, based on this difference, the FS analysis method can be used to distinguish the internal fault, EFLS and EFOS.

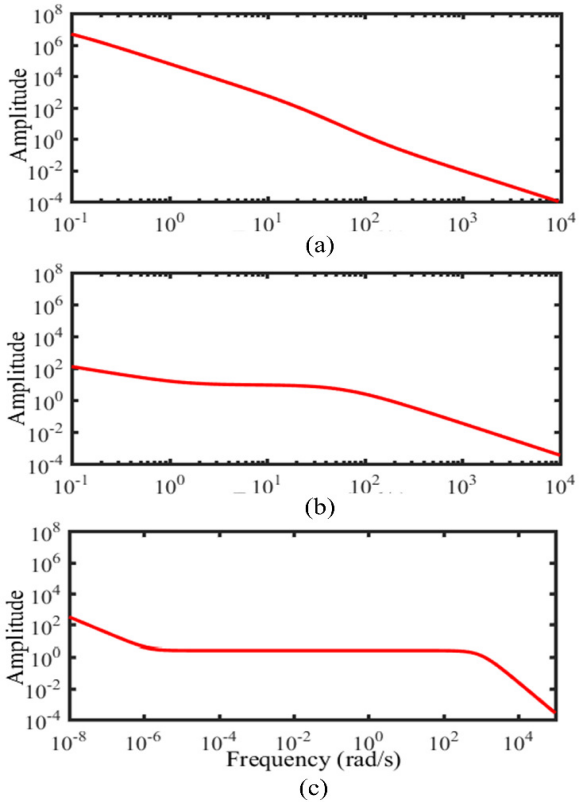

Fig.3. Amplitude frequency characteristics
(a)Opposite side fault; (b) Local side fault; (c) Internal fault

3. HVDC internal and external fault criterion

The fault simulation of the unipolar HVDC system is carried out. A fault occurs at 1 s and is removed after 0.05s.

4 DC currents are measured at the inverter side, which are EFOS, EFLS, the internal fault and the normal operating condition. After decomposition of the DC signals by Fourier analysis, the FS characteristics of the DC currents are obtained and shown in Fig.4.

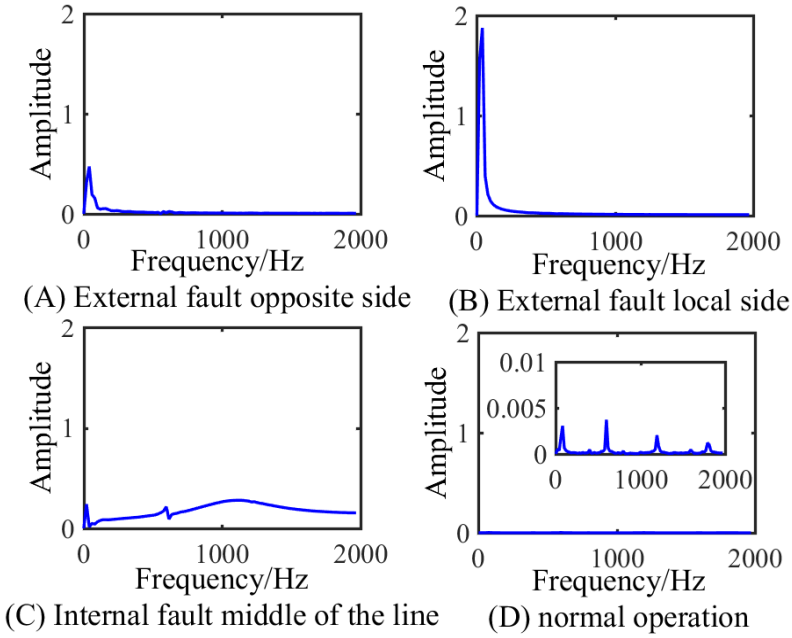

Fig.4. Frequency spectrum characteristics

In Fig.4, A, B, C and D denote the FS curves of the EFOS, EFLS, the internal fault and the normal operation respectively. In this paper, the FS of an internal fault on the middle of the DC transmission line is chosen as the EFS of the internal fault, because of the long transmission distance, the internal fault occurring close to the rectifier and inverter side leads to slightly different FS between them. Therefore, for internal faults, it is appropriate to select the FS of the middle position of the DC line as the internal fault EFS.

EFS characteristics are intrinsic for the DC line. And from qualitative analysis, the following characteristics can be got:

(1) For the external fault, the frequency components are relatively mainly concentrated in the low frequency components. The high frequency components decay is higher for the EFOS than the EFLS. It is mainly due to the differences of physical boundary;

(2) For the internal fault and normal operation, since the physical boundaries do not contain smoothing reactor and DC filter, the frequency band contains both high frequency components and low frequency components. The FS of the internal fault is expected to be greatly irregular as shown in the figure. The FS of normal operation is fairly regular and mainly contains 4 small frequency components.

These intrinsic FS characteristics can be used as criteria for judging the internal and external faults. In this paper, Pearson correlation coefficient method [20] is used to discriminate the four cases. For two sets of data $X=\{x_1, x_2, \ldots, x_n\}$ and $Y=\{y_1, y_2, \ldots, y_n\}$, the correlation coefficient is defined as:

$$r(X,Y)=\frac{\sum_{i=1}^{n}(x_i-\frac{1}{n}\sum_{j=1}^{n}x_j)(y_i-\frac{1}{n}\sum_{j=1}^{n}y_j)}{\sqrt{\sum_{i=1}^{n}(x_i-\frac{1}{n}\sum_{j=1}^{n}x_j)^2}\sqrt{\sum_{i=1}^{n}(y_i-\frac{1}{n}\sum_{j=1}^{n}y_j)^2}} \tag{4}$$

where (X,Y) is the correlation coefficient of signals X and Y ; the range is $r(X,Y)\in[-1,+1]$, here -1 indicates a negative correlation between the two signals, +1 means complete correlation and 0 indicates totally unrelated. The size of the value r

represents the degree of similarity between the two signals. The larger the value is, the more similar the two signals are. From the above four FS, a group of EFS vectors is formed as:

$$[a(x_1, x_2, \cdots, x_N), b(x_1, x_2, \cdots, x_N), c(x_1, x_2, \cdots, x_N), d(x_1, x_2, \cdots, x_N)] \quad (5)$$

where *a*, *b*, *c* and *d* denote the FS data of the EFOS, EFLS, the internal fault and the normal operation respectively; *N* is the dimension of the data for each FS. When system fault happens, the transient DC current is analyzed by discrete Fourier analysis to obtain the DC current FS. Then the correlation coefficients between FS and EFS are calculated and a set of vectors is obtained (r_1, r_2, r_3, r_4). r_1, r_2, r_3, r_4 refer to the EFOS, EFLS, the internal fault and the normal operation respectively. The larger the value is, the greater the similarity is. The type of fault can be judged by the correlation coefficient, the maximum value of the correlation coefficient is the product of judgment.

4. Starting condition of fault discrimination program

In order to improve the reliability of the discriminant program, this paper set a threshold value defined by the size of the dynamic permutation entropy ratio to entable the start and stop of the discriminant program.

Permutation entropy is a mean entropy parameter to measure the complexity of one-dimensional time-series data [21]. It can better reflect the tiny change of time series data and has high robustness which mainly used in meteorology, medical and mechanical fault prediction. The following introduces its basic principle.

Suppose $\{X(i), i=1, 2, 3\ldots,n\}$ is a time-series signal. The permutation entropy (PE) of the different symbol sequences of the time series data is defined as [21]:

$$H_p(m) = -\sum_{j=1}^{k} P_j \ln P_j \quad (6)$$

when $P_j = 1/m!$, $H_p(m)$ has the maximum value of $\ln(m!)$. For the purpose of convenience, normalization is usually used as follows:

$$H_p = H_p(m)/\ln(m!) \quad (7)$$

where H_p belongs to $0 \leqslant H_p \leqslant 1$ indicating the random degree of time series data of $[X(i), i = 1, 2, 3, \cdots, n]$. The smaller the value of H_p is, the more regular the time series data is. Conversely, the time series data are closer to random if H_p is small. The value of H_p reflects and magnifies small changes in the time series data.

The permutation entropy is the mean entropy parameter to measure the complexity of one-dimensional time series data. The arrangement entropy is very small when the system is running normally and the entropy value is very large when the system is in a state of fault. Hence, the system fault and normal operation can be determined by comparing the entropy values. Because the permutation entropy has the capability to amplify tiny mutation, this method is almost free from the influence of high resistance ground fault. The size of the permutation entropy is affected by m and τ. In order to avoid the influence of m and τ, and realize the quantitative analysis of system fault, the permutation entropy difference ratio is defined as:

$$k_2 = \frac{pec(I_d(t_1 + nT/2, t_1 + 3nT/2)) - pec(I_d(t_1, t_1 + nT))}{pec(I_d(t_1, t_1 + nT))} \quad (8)$$

where *pec* is the permutation entropy of the DC current; T is the sampling period. In this paper, the sampling period is 250 microseconds; I_d (t_1, t_1+nT) is time series data value of DC current from t_1 to t_1+nT.

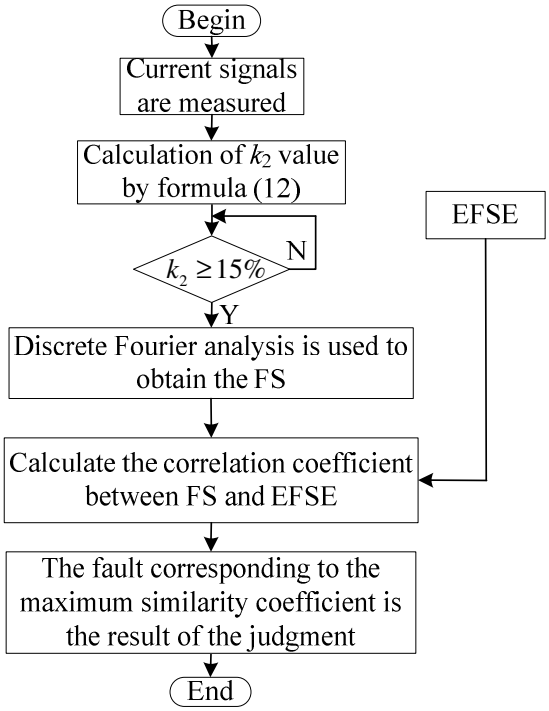

Fig.5. DC internal and external faults judging process

When the system is in normal running state, the measurement error and noise or other random factors, the value k_2 is usually in the range of 5%. When the system is in fault state, the value of k_2 will certainly go beyond 10%. Considering a safe margin, this paper takes the threshold as 15%. When the value exceeds the threshold, it can be judged that the system has a fault. Finally, the logical judgment process of the internal and external faults is shown in Fig.5.

5. Comparison with existing protection schemes

5.1. Characteristics of the proposed method

The proposed algorithm is shown using a flowchart in Fig.8. The protection logic mainly has two stages. The first stage is fault threshold calculation using the permutation entropy difference ratio criterion. Due to the criterion is defined by the ratio, therefore, it not affected by the strength of the actual fault signal. The second stage is correlation coefficient calculation. According to the principle of similarity, it only reflects the similarity of the shape of the two signals, so it not affected by the fault grounding resistance. Compared with the single-end time-domain based travelling wave protection [22, 23], which use the rate of voltage change as the criterion, the protection principle of the proposed method is entirely different. The proposed method gets its inherent advantages. Compared with two-end signal-based protection [24], which can identify the internal faults with satisfactory selectivity and sensitivity, however, the speed and reliability of two-end signal-based methods are insufficient due to the requirement of data exchange. The proposed method

out-perform other methods as it only needs single-end signals, easy to achieve and has high reliability.

5.2. Comparison of detection speed

According HVDC transmission line protection recently published in [25], the sum of all time delays before the current breaking begins is:

$$t_{op1} = t_{CB1} + t_{meas1} + t_{process1} \tag{9}$$

where t_{CB1} the inherent operation time of circuit breaker; t_{meas1} is the measurement delay time; $t_{process1}$ is the calculation time of protection algorithm.

The sum of all time delays before the current breaking begins proposed method in this paper is:

$$t_{op2} = t_{CB2} + t_{meas2} + t_{process2} \tag{10}$$

where t_{CB2}, t_{meas2} and $t_{process2}$ indicate the same meaning as t_{CB1}, t_{meas1} and $t_{process1}$, respectively. Here t_{CB2} is equal to t_{CB1}, t_{meas2} is equal to t_{meas1}, $t_{process2}$ is composed of calculated time of k_2 and correlation coefficient, which is about 1 ms, almost equal to $t_{process1}$. By comparing t_{op1} and t_{op2}, we can see that the proposed method has almost the same action time as the above method, so it can meet the requirements of the quick action.

6. Simulation

6.1. Unipolar DC transmission system simulation

Taking the standard CIGRE model as an example, the system structure diagram is shown in Fig.1.

(1) Simulation verification under ideal conditions

Setting up faults at different locations respectively. External fault position at F_1(F_1) in the Fig.1; internal fault position close to the rectifier (F_{d1}); internal fault position at the middle of DC line (F_{d2}); internal fault position close to the inverter (F_{d3}); external fault position at F_3 (F_3) in the Fig.1; DC power fluctuation but without fault (P_1); normal operation (N_1). All faults are set up at 2s and eliminated after 0.05s.

Table1. Simulation results

Operation situation	k_2	r_1	r_2	r_3	r_4
F_1	0.36	***0.9675***	0.0692	-0.3646	0.2800
F_{d1}	0.42	-0.3001	-0.3027	***0.9494***	0.6038
F_{d2}	0.28	0.0018	-0.2015	***0.9082***	0.8374
F_{d3}	0.54	-0.2748	-0.2855	***0.3138***	-0.0794
F_3	0.29	0.1534	***0.9427***	-0.3874	0.2901
P_1	0.02	0.2437	0.1228	-0.1007	***1.0000***
N_1	0.01	0.3253	0.1985	-0.2092	***0.9110***

The correlation values with highest magnitudes are highlighted in the simulation results of Table 1. It can be found that this method can accurately identify the internal fault, EFLS and EPOS.

The EFS eigenvector of the unipolar system is obtained by the fault occurs at 1s, while at the time of simulation verification the fault we set at 2 s. According to the calculation results of Table 1, correlation coefficient method is not affected by the time of fault occur. EFS of internal fault is obtained by the fault occurs on the middle position of DC line, while during simulation verification, the fault is set at different position. The simulations

get the same results. Hence the internal fault discrimination method is not affected by the fault position and the proposed method is proved to be robust.

(2) The influence of noise

The measured signals in power systems usually contain noise. In order to simulate real signals, in this paper, noise is added to the original measurement signal to form a real signal that contains measurement noises. The measurement noises following Gauss distribution is added and the standard deviation is set to 0.005 (p.u.) [26].

Table 2. Simulation results

Operation situation	k_2	r_1	r_2	r_3	r_4
F_1	0.48	***0.9175***	0.1820	-0.4091	0.2871
F_{d1}	0.44	-0.3781	-0.4157	***0.9072***	0.5940
F_{d2}	0.35	0.0579	-0.3870	***0.9763***	0.7539
F_{d3}	0.50	-0.2865	-0.2841	***0.3012***	-0.0892
F_3	0.39	0.1873	***0.9531***	-0.3961	0.2813
P_1	0.09	0.2863	0.1763	-0.1901	***0.9842***
N_1	0.03	0.3438	0.1875	-0.2891	***0.9092***

From the simulation results of Table 2, it can be found that this method is robust and able to tolerant measurement noises in DC current signals.

(3) Influence of fault grounding resistance

In order to analyze the influence of grounding resistance on fault diagnosis results, this paper set different transition resistances at two positions in the DC line respectively. The distances are1/4 (F_{d11}) and 3/4 (F_{d22}) from the rectifier side with respect to the full length of DC line, and the resistance respectively is 100, 500 and 800Ω. The FS under different transition resistances is shown in Fig.6 (a) and Fig.6 (b).

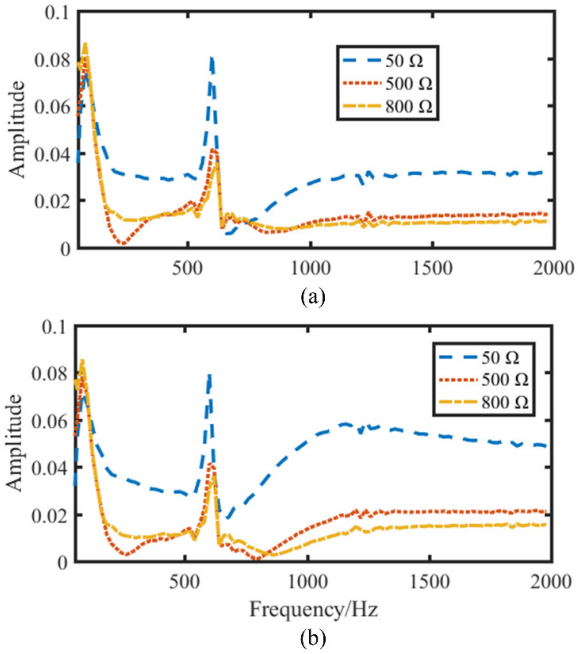

Fig.6. Amplitude frequency curves of different transition resistance
(a)Location at Fd_{11}; (b) Location at Fd_{22}

It can be seen from Fig.6 (a) and Fig.6 (b) that, under the influence of transition resistance, only amplitude of frequency characteristic will be changed, and the shape of the

whole amplitude frequency characteristic curve will hardly be affected. It is proved that the method is almost free of the influence of transition resistance.

(4) Influence of fault location

High resistance ground fault is fixed at 500Ω. Different fault locations are simulated and the results are shown in table 3.

Table 3. Simulation results

Operation situation	k_2	r_1	r_2	r_3	r_4
F_1	0.32	***0.8723***	0.0781	-0.3571	0.2691
F_{d1}	0.42	-0.3315	-0.3045	***0.9053***	0.6324
F_{d11}	0.37	-0.2123	-0.4141	***0.9102***	0.7271
F_{d2}	0.30	0.0082	-0.2167	***0.9184***	0.8439
F_{d22}	0.36	0.0019	-0.3491	***0.9721***	0.8081
F_{d3}	0.58	-0.2684	-0.2831	***0.3321***	-0.0836
F_3	0.29	0.1848	***0.9120***	-0.3941	0.2957

6.2. AC/DC parallel transmission system

Two-area four-machine AC/DC parallel system is built as an example of complex system. The system architecture is shown in Fig.7. There are two generators in each area 1 and area 2, detailed parameters of the system can be found in reference [27].

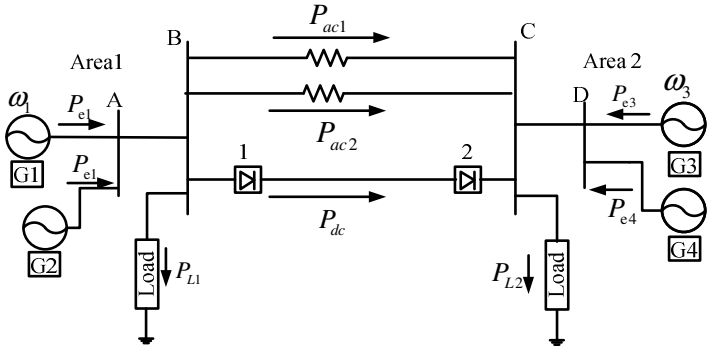

Fig.7. DC transmission system structure

In order to verify the effectiveness and robustness of the proposed method in this paper, normal operation conditions and various types of faults are simulated on two-area four-machine AC/DC parallel system. Under normal operation, the influence of system structure and quantity of power supply on the result is simulated and analyzed; under abnormal operation, the influence of fault position and transition resistance on the result are simulated and analyzed.

(1) System structure: normal grid structure (N_{s1}), resection of an AC transmission line (N_{s2});

(2) The number of generators: four generators (N_{v1}), two generators (N_{v2})-remove a generator at the sending end and the receiving end respectively.

(3) The location of the fault: located at the external opposite side (D_{p1}), internal closed to rectifier (D_{p2}), the middle position of the DC line (D_{p3}), internal closed to inverter (D_{p4}) and the external local side (D_{p5});

(4) The fault transition resistance is set to two types: metal grounding fault resistance is 0.005Ω(R_1), high resistance ground fault transition resistance is 50Ω(R_2).

Table 4. Simulation results

Operation situation	k_2	r_1	r_2	r_3	r_4
N_{s1},N_{v1}	0.02	-0.1461	-0.4720	-0.3717	***0.9982***
N_{s1},N_{v2}	0.01	0.1108	-0.3213	-0.1000	***0.9216***
N_{s2},N_{v1}	0.03	-0.1486	-0.5068	-0.3677	***0.9905***
N_{s2},N_{v2}	0.02	-0.3590	-0.0650	-0.4575	***0.6116***
D_{p1},R_1	0.46	***1.0000***	0.9512	0.9914	0.0185
D_{p1},R_2	0.49	***0.9992***	0.7621	0.7930	0.0241
D_{p2},R_1	0.58	0.7933	0.7636	***0.9979***	0.0080
D_{p2},R_2	0.51	0.7416	0.8398	***0.9148***	0.0644
D_{p3},R_1	0.26	0.7910	0.7630	***0.9999***	-0.0070
D_{p3},R_2	0.32	0.7515	0.8551	***0.9268***	0.0630
D_{p4},R_1	0.30	0.7890	0.7631	***0.9955***	-0.0081
D_{p4},R_2	0.31	0.7576	0.8652	***0.9385***	0.0528
D_{p5},R_1	0.36	-0.1779	***0.8056***	-0.0778	-0.3413
D_{p5},R_2	0.47	-0.2907	***0.7249***	-0.2028	-0.2616

Based on the above simulation analysis, it can be concluded that the proposed method is less affected by the structure of the grid, transition resistance and other factors. It can meet the requirements of selectivity and robustness.

7. Conclusion

A novel fast identification method of internal and external faults of HVDC transmission line based on FS correlation is proposed in this paper. There are different physical boundaries between the internal and external faults, causing different FS characteristics obtained by the discrete Fourier analysis. Simulation analysis is carried out on the unipolar DC transmission system as well as AC/DC parallel transmission system under different conditions and various fault types. The results verify the feasibility and robustness of the proposed method. Some meaningful conclusions are obtained as follows:

(1) Under the action of DC filter and smoothing reactor, the frequency components of a DC current signal have a characteristic difference. In normal operation, the DC current contains both high frequency and low frequency. When external fault happens, the frequency component of DC current is relatively concentrated to single-frequency; the degree of attenuation of the opposite side is higher than that of the local side. The component of DC current has no obvious regularity in the internal fault.

(2) The time of system fault, system capacity, power network structure and transition resistance have little influence on this method, showing its robustness and promising application potentials;

(3) This method only needs single information DC current. It is simply and easy to implement, and can meet the requirements of selectivity and speed.

Therefore, this research results have some reference value for DC line fault protection.

Acknowledgment

This work was jointly supported by the National Natural Science Foundation of China (51607158), Maker space incubation project of Zhengzhou University of light industry (2020ZCKJ206).

References

[1] X. C. Huang, P. He, G. Z. Cui, et al., “Review, development and suggestion of Chinese smart grid,” Journal of light industry, 2016, 31(2) :54-64.

[2] B. H. Zhang, F. Kong, S. Zhang, et al., "Technical development of non-unit protection devices based on transient signals for HVDC transmission lines,"Proc. CSEE.2013, 33(4):179-185.
[3] M. Farshad, J. Sadeh, "A novel fault-location method for HVDC transmission lines based on similarity measure of voltage signals," IEEE Trans. Power Del. 2013, 28(4):2483-2490.
[4] M. Li, Z. X. Cai, X. H. Li, "Study on the propagation characteristics of traveling waves in HVDC transmission lines on the basis of analytical method," Proc. CSEE. 2010, 30(25):94-100.
[5] J. S. Wang, H. Y. Li, D. M. Cao, et al., "Discussion on some problems in bi-pole area of ±800kV UHVDC system protect," AEPS. 2006,30 (23) :85-88.
[6] M. Li, Z. X. Cai, Q. Z. Sun, et al., "Study on the dynamic performance characteristics of HVDC control and protections for the HVDC line fault," in Proc. Power Energy Soc. Gen. Meeting, 2009, pp.1-5.
[7] J. L. Suonan, J. K. Zhang, Z. B. Jiao, et al., "Distance protection for HVDC transmission lines considering frequency-dependent parameters," IEEE Trans. Power Del. 2013,28(2): 723–732.
[8] D. Naidoo, N. M. Ijumba, "HVDC line protection for the proposed future HVDC systems," Proc. IEEE Power con Conf., November 2004, pp. 1327–1332.
[9] F. Kong, Z. G. Hao, S. Zhang, et al., "A novel traveling-wave-based main protection scheme for 800 kV UHVDC bipolar transmission lines," IEEE Trans. Power Deli. 2016,31(5) :2159–2168.
[10] H. C. Shu, X. C. Tian, J. Dong et al., "Identification between internal and external faults of ±800kV HVDC transmission lines based on voltage correlation," Proc. CSEE. 2012, 32(4):151-160.
[11] H. C. Shu, X. C. Tian, J. Dong et al., "Recognition Method of HVDC Transmission Line Fault Based on Multi-fractal Spectrum," Transactions of China Electrotechnical Society, 2013, 28(1) :251-258.
[12] S. L. Chen, R. K. Cao, G. H. Bi et al., "Distinguish Faults Located Inside/Outside Protection Zone of UHVDC Transmission Line by Multi-Resolution Singular Spectrum Entropy and Support Vector Machine," Power System Technology, 2015, 39(4):989-994.
[13] X. L. Liu, A. H. Osman, and O. P. Malik, "Hybrid traveling wave/ boundary protection for monopolar HVDC line," IEEE Trans. Power Del. 2009, 24(2):569–578.
[14] H. C. Shu, K. Z. Liu, S. Q. Zhu, et al., "±800 kV UHVDC transmission line protection based on single end electrical transient protection," Proc. CSEE. 2010, 30(31):108–117.
[15] H. C. Shu, X. C. Tian, Y. T. Dai, "The identification of internal and external faults for ±800 kV UHVDC transmission line based on S-transform of the polarity wave," in Proc. Int. Conf. Image Signal Process., 2010, pp. 3060–3063.
[16] X. D. Zheng, N. L. Tai, J. S. Thorp, et al., "A transient harmonic current protection scheme for HVDC transmission line," IEEE Trans. Power Del. 2012, 27(4) :2278–2285.
[17] G. B. Song, X. Chu, S. P. Gao, et al., "A new whole line quick-action protection principle for HVDC transmission lines using one-end current," IEEE Trans. Power Del. 2015, 30(2):599–607.
[18] M. You, B. H. Zhang, R. F. Cao, et al., "Study of Non-unit transient-based protection for HVDC transmission lines, in APPEEC," Wuhan, China, 2009, pp. 108-113.
[19] Zhang J, XU Z, WANG F, et al. "TLS-ESPRIT Based Method for Low Frequency Oscillation Analysis in Power System." Automation of Electric Power Systems, 2007, 20: 84-88.
[20] Benesty J, Chen J, Huang Y, et al. Pearson correlation coefficient[M]//Noise reduction in speech processing. Springer, Berlin, Heidelberg, 2009: 1-4.
[21] C. S. Li, T. Q. Liu, X. Y. Li, et al., "Power System Fault Signal Analysis Based on Permutation Entropy Algorithm, Journal of University of Electronic Science and Technology of China," 2015, 44(2): 233-238.
[22] Li, Z. Cai, X. Li, et al., "Analysis of influence factors and improvement of traveling wave protections for HVDC line, Autom." Electr. Power Syst. (China), 2010, 34 (10):76–80.
[23] K. Han, Z. Cai, M. Xu, et al., "Dynamic characteristics of characteristic parameters of traveling wave protection for HVDC transmission line and their setting," Power Syst. Tech. (China), 2013, 37(01): 255–260.
[24] S. Gao, G. Song, Z. Ma, et al., "Novel pilot protection principle for high voltage direct current transmission lines based on fault component current characteristics," IET Gener. Transm. Distrib., 2015, 9(5):468–474.
[25] D. Tzelepis, A. DyŚko, G. Fusiek, et al., "Single-Ended Differential Protection in MTDC Networks Using Optical Sensors," IEEE Trans. Power Del. 2017, 32(3):1605-1615.
[26] C. S. L, T. Q. Liu, X. Y. Li, et al., "Data Fusion Method of WAMS/SCADA Hybrid Measurements in Power System State Estimation," High Voltage Engineering, 2013, 39(11): 2686-2691.
[27] C. S. L, T. Q. Liu, L. B. Liu, et al., "Aauto-disturbance rejection controller of multi-HVDC," Transactions of China Electrotechnical Society, 2015, 30(7):10-17.